ELSEVIER

Journal of Nuclear Materials 313–316 (2003) 1041–1045

journal of nuclear materials

www.elsevier.com/locate/jnucmat

Asymmetry of dense divertor plasmas influenced by thermoelectric potential and charge-exchange momentum loss

N. Hayashi [a,*], T. Takizuka [a], M. Hosokawa [b], K. Shimizu [a]

[a] *Naka Fusion Research Establishment, Japan Atomic Energy Research Institute, 801-1 Mukouyama, Naka, Ibaraki 311-0193, Japan*

[b] *Research Organization for Information Science & Technology, Tokai, Ibaraki 319-1106, Japan*

Abstract

Asymmetric equilibria of divertor plasmas influenced by the thermoelectric potential and the momentum loss due to the charge-exchange collisions have been studied by using a five-point model. The momentum loss becomes large when the divertor plasma temperature decreases below about 10 eV. The increase of the pre-sheath potential due to the momentum loss compensates the reduction of the sheath potential at the low-temperature side of an asymmetric equilibrium. Through the change of the pre-sheath potential, the momentum loss has a stabilizing effect on the thermoelectric instability and mitigates the asymmetry at the high-density divertor regime. The momentum loss at the low-temperature and high-density side divertor is effective to lower the temperature at the high-temperature side divertor.
© 2003 Elsevier Science B.V. All rights reserved.

Keywords: Divertor asymmetry; Thermoelectric instability; SOL current; Charge-exchange; Momentum loss; Divertor modeling

1. Introduction

Between two divertor regions at either end of an open magnetic field line, plasma parameters, such as temperature, are generally different. A scrape-off layer (SOL) current driven by the thermoelectric sheath potential is considered to be one of the causes of the asymmetry. The SOL current increases the temperature asymmetry by driving a convective electron heat toward the hotter divertor plasma (see Fig. 1). This unstable behavior is called thermoelectric instability [1]. We have studied the equilibrium and the stability with the SOL current by using a five-point model which does not take account of the momentum loss [2–4]. When the divertor plasma temperature decreases below a threshold value in the dense plasma with the high-recycling state, the symmetric equilibrium is destabilized and two stable asymmetric equilibria appear [2,3]. When the asymmetry is induced externally by the biasing and the recycling, the dependence of the divertor plasma on the bias voltage and recycling has a bifurcated structure [4]. In a dense and cold divertor side of an asymmetric equilibrium (see Fig. 1), the momentum loss due to the charge-exchange (CX) becomes important and the detached divertor plasma may be easily formed.

In this paper, we study the asymmetric equilibria influenced by the thermoelectric potential and the CX momentum loss by using the five-point model. A simple model for the CX momentum loss has been developed and introduced into the five-point model.

2. Five-point model with the momentum loss due to the charge-exchange

Fig. 1 shows a geometry of the model. The detailed model is described in Refs. [2,3]. The model is based on fluid equations, i.e., particle, momentum, energy,

* Corresponding author. Tel.: +81-29 270 7518; fax: +81-29 270 7419.

E-mail address: hayashin@fusion.naka.jaeri.go.jp (N. Hayashi).

0022-3115/03/$ - see front matter © 2003 Elsevier Science B.V. All rights reserved.
PII: S0022-3115(02)01534-9

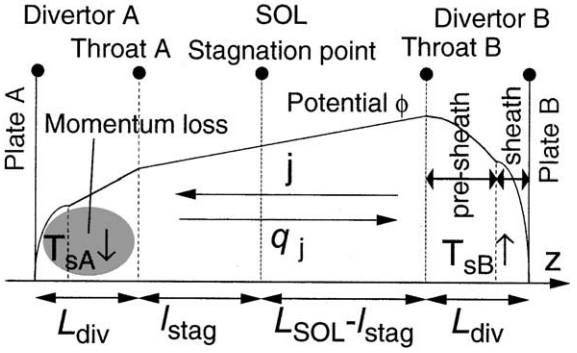

Fig. 1. Geometry for five-point model where z denotes the length along the magnetic field. The thermoelectric sheath potentials in asymmetric SOL-divertor plasma with $T_{sA} < T_{sB}$ drive SOL current j. Heat flux q_j by j causes the thermoelectric instability.

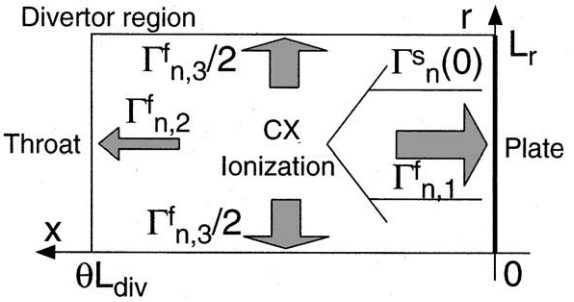

Fig. 2. Geometry for model of CX momentum loss where x and r are poloidal and radial direction, respectively. Flux $\Gamma^s_n(0)$, $\Gamma^f_{n,1}$, $\Gamma^f_{n,2}$ and $\Gamma^f_{n,3}$ denote slow neutrals released from divertor plate, fast neutrals escaping to plate, to divertor throat and to radial directions, respectively.

generalized Ohm's law and current equations. Currents perpendicular to the magnetic field are not taken into account. The momentum equation and generalized Ohm's law are given as

$$\frac{\partial}{\partial z}(mnv^2 + 2nT) = -S_m,$$
$$\frac{\partial \phi}{\partial z} = -\eta j + \frac{\alpha}{e}\frac{\partial T}{\partial z} + \frac{1}{en}\frac{\partial nT}{\partial z}, \quad (1)$$

where $\alpha = 0.71$ and z denotes the length along the magnetic field. Quantities, n, v, T, S_m, ϕ, j and η, denote the plasma density, the flow velocity, the temperature ($T = T_e = T_i$), the momentum sink, the electrostatic potential, the SOL current density parallel to the magnetic field, and the electric resistivity, respectively. In the divertor plasma region, the energy sink, W_{div}, is assumed to be $W_{div} = -k\Delta E S_N$ where $k = 4$, $\Delta E = 13.6$ eV and S_N denotes the plasma particle source due to ionization of neutrals. The particle flux Γ_s flowing into the plate are given by $\Gamma_s = n_s\sqrt{4T_s/m}$ based on the results of a particle simulation code PARASOL [5]. The subscript 's' denotes the sheath entrance.

Neutrals in divertor plasmas cause the momentum loss of the parallel plasma flow through the CX collisions. Fig. 2 shows a geometry of the CX momentum loss model where x and r denote the poloidal and the radial direction, respectively. We consider two steps for the neutral transport, (1) slow neutrals with a velocity of $v_0 = \sqrt{E_n/m}$ released from divertor plates to the x direction have the ionization and CX collisions with plasmas, (2) fast neutrals produced by the CX collisions are randomly directed with a thermal velocity of $v_{th} = \sqrt{T_s/m}$. The momentum is transfered from the plasma to the fast neutrals and is lost if the fast neutrals escape from the plasma. The momentum direction of the parallel plasma flow is mainly toroidal (perpendicular to the plane of Fig. 2). The particle flux of the fast neutrals with the toroidal momentum escapes from the plasma to the poloidal or the radial direction. This model is developed from Harrison's model [6] which only takes account of the returning particle flux to the plate. The flux Γ^s_n of slow neutrals is given by, $\Gamma^s_n(x) = \Gamma^s_n(0)\exp(-x/\lambda)$, where $1/\lambda = 1/\lambda_{CX} + 1/\lambda_i$, $\lambda_{CX} = v_0/n_s\langle\sigma v\rangle_{CX}$ denotes the mean free path for CX, and $\lambda_i = v_0/n_s\langle\sigma v\rangle_i$ for ionization. The fast neutral source of $\Gamma^s_n(x)/\lambda_{CX}$ is produced and the fast neutrals move isotropically to the divertor plates, to the divertor throat or to the radial direction. Motions of the fast neutrals can be treated as a diffusive process. The scale length, λ', of the diffusion is expressed as $\lambda' = \sqrt{\lambda'_{CX}\lambda'_i}$ where $\lambda'_{CX} = v_{th}/n_s\langle\sigma v\rangle_{CX}$ and $\lambda'_i = v_{th}/n_s\langle\sigma v\rangle_i$. The flux of the fast neutrals returning to the divertor plates, $\Gamma^f_{n,1}$, is derived as

$$\Gamma^f_{n,1} = \frac{\Gamma^s_n(0)}{4\lambda_{CX}}\int_0^{\theta L_{div}} \exp(-x/\Delta_1)\,dx = \frac{\Gamma^s_n(0)}{4}\frac{\Delta_1}{\lambda_{CX}}\left(1 - \exp\left(-\frac{\theta L_{div}}{\Delta_1}\right)\right), \quad (2)$$

where $1/\Delta_1 = 1/\lambda + 1/\lambda'$. In the same way as $\Gamma^f_{n,1}$, the flux to the divertor throat, $\Gamma^f_{n,2}$, is given as

$$\Gamma^f_{n,2} = \frac{\Gamma^s_n(0)}{4}\frac{\Delta_2}{\lambda_{CX}}\exp\left(-\frac{\theta L_{div}}{\lambda'}\right)\left(1 - \exp\left(-\frac{\theta L_{div}}{\Delta_2}\right)\right), \quad (3)$$

where $1/\Delta_2 = 1/\lambda - 1/\lambda'$. The flux escaping to the radial direction, $\Gamma^f_{n,3}$ (see Fig. 2), is given as

$$\Gamma^f_{n,3} = \frac{\Gamma^s_n(0)}{2}\frac{\lambda}{\lambda_{CX}}\left(1 - \exp\left(-\frac{\theta L_{div}}{\lambda}\right)\right) \times \frac{\lambda'}{L_r}\left(1 - \exp\left(-\frac{L_r}{\lambda'}\right)\right), \quad (4)$$

where L_r is a radial width of the divertor plasma. The fast neutrals returning to the plate are assumed to be released again as slow neutrals. A total particle flux

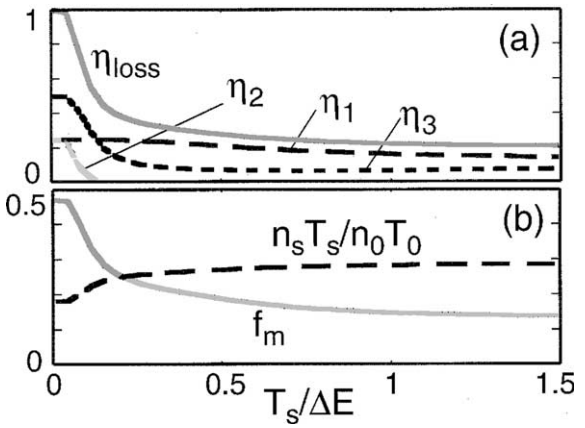

Fig. 3. Values of (a) $\eta_{\rm loss}$, η_j $(j = 1, 2, 3)$, (b) momentum loss $f_{\rm m}$ and $n_{\rm s}T_{\rm s}/n_0T_0$ as a function of $T_{\rm s}$ normalized by $\Delta E = 13.6$ eV where $n_{\rm s}T_{\rm s} = 200$ Pa ($n_{\rm s} \approx 9 \times 10^{19}$ m^{-3} at $T_{\rm s} = \Delta E$), $E_{\rm n} = 0.01$ eV and $L_{\rm r} = 0.1$ m.

escaping from the plasma is given as, $\eta_{\rm loss}\Gamma^{\rm s}_{\rm n}(0) = \eta_{\rm loss}\theta\Gamma_{\rm s}/(1-\eta_1)$, where $\eta_{\rm loss} = \sum_{j=1}^{3}\eta_j$ and $\eta_j = \Gamma^{\rm f}_{{\rm n},j}/\Gamma^{\rm s}_{\rm n}(0)$.

The momentum equation integrated from a stagnation to the divertor plate is given as

$$6n_{\rm s}T_{\rm s} - 2n_0T_0 = -\int_{\rm div} S_{\rm m}\,{\rm d}z \approx -c_{\rm m}mv_{\rm s}\Gamma_{\rm s}\frac{\eta_{\rm loss}}{1-\eta_1} = -4c_{\rm m}n_{\rm s}T_{\rm s}\frac{\eta_{\rm loss}}{1-\eta_1}, \quad (5)$$

where $c_{\rm m}$ is given as a parameter with a range of $0 \leqslant c_{\rm m} \leqslant 1$ to investigate the effect of the momentum loss. A ratio of the divertor plasma pressure, $n_{\rm s}T_{\rm s}$, to the stagnation one, n_0T_0, is given as

$$\frac{n_{\rm s}T_{\rm s}}{n_0T_0} = \frac{1}{3}(1-f_{\rm m}), \quad f_{\rm m} = \frac{2n_{\rm s}T_{\rm s}}{n_0T_0}c_{\rm m}\frac{\eta_{\rm loss}}{1-\eta_1}. \quad (6)$$

Fig. 3 shows the dependence of (a) $\eta_{\rm loss}$, η_j $(j = 1, 2, 3)$, (b) the ratio of the momentum loss to the stagnation pressure, $f_{\rm m}$, and $n_{\rm s}T_{\rm s}/n_0T_0$ on $T_{\rm s}/\Delta E$ where $n_{\rm s}T_{\rm s} = 200$ Pa, $E_{\rm n} = 0.01$ eV and $L_{\rm r} = 0.1$ m. For $T_{\rm s}/\Delta E < 1$ (about 10 eV), $\eta_{\rm loss}$ increases due to the decrease in the ionization probability. When $T_{\rm s}/\Delta E$ decreases near zero, $\eta_{\rm loss}$ largely increases and reaches to unity, i.e., the momentum loss, $f_{\rm m}$, becomes large and the pressure ratio, $n_{\rm s}T_{\rm s}/n_0T_0$, decreases. The characteristic of the increase in $f_{\rm m}$ at low $T_{\rm s}$ is similar for various values of $n_{\rm s}T_{\rm s}$, $E_{\rm n}$ and $L_{\rm r}$.

3. Results

The equilibria and their stability of SOL and divertor plasmas are examined numerically (see Refs. [2,3]). The particle flux amplification factor R defined by the ratio of $\Gamma_{\rm s}$ to the particle flux at the divertor throat is an input parameter and characterizes a recycling strength in the divertor region. The potential difference between two divertor plates 'A' and 'B' (see Fig. 1) is set at zero for electrically grounded plates. Other parameters are chosen to be similar to typical parameters in JT-60U: the total particle and heat flows from the core to the SOL plasma are $\Phi_{\rm sep} = 5 \times 10^{22}$ s^{-1} and $Q_{\rm sep} = 10$ MW, respectively. The radial particle and thermal diffusivities are chosen as $D_\perp = 1$ m^2/s and $\chi_\perp = 2$ m^2/s, respectively. Geometrical parameters are $L_{\rm SOL} = 100$ m, $L_{\rm div} = 4$ m in Fig. 1, and the pitch of the magnetic field $\theta = 0.06$.

3.1. Effect of the momentum loss on the asymmetric equilibrium

Fig. 4 shows the dependence of stable equilibrium values of (a) $T_{\rm s}/\Delta E$ and (b) the momentum loss, $f_{\rm m}$, on R for various $c_{\rm m}$ values ($c_{\rm m} = 0, 0.5, 1$). The values of $c_{\rm m} = 0$ and 1 correspond to cases without and with the momentum loss, respectively. In Fig. 4, the divertor 'A' is the low-$T_{\rm s}$ side and 'B' is the high-$T_{\rm s}$ side. The symmetric equilibrium becomes unstable due to the thermoelectric instability and the stable asymmetric equilibria appears for $R \geqslant 18$. Without the momentum loss ($c_{\rm m} = 0$), the asymmetry increases with R. When R increases near $R = 40$, $T_{\rm sB}$ largely increases and $T_{\rm sA}$ decreases near zero. The large increase in $T_{\rm sB}$ for $c_{\rm m} = 0$ is found even in the case without the SOL current ($j = 0$) and explained as follows. Without the current, the

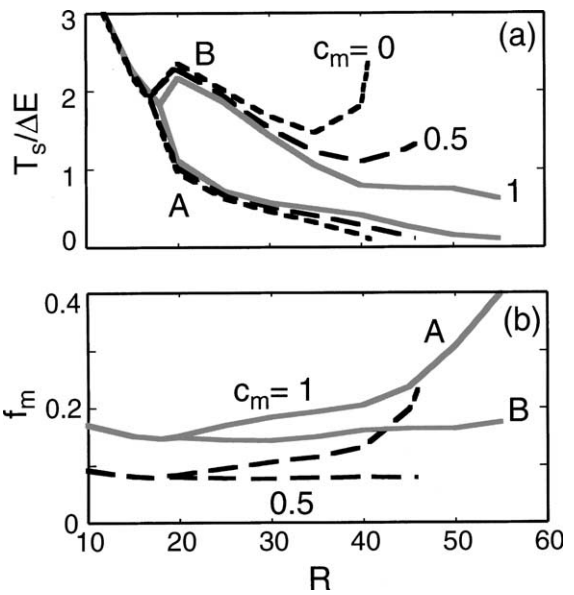

Fig. 4. Dependence of stable equilibrium values of (a) $T_{\rm s}/\Delta E$ and (b) momentum loss $f_{\rm m}$ on R for $c_{\rm m} = 0$, 0.5, 1. Here, divertor 'A' is low-$T_{\rm s}$ side and 'B' is high-$T_{\rm s}$ side as illustrated in Fig. 1. Values of $c_{\rm m} = 0$ and 1 correspond to cases without and with momentum loss, respectively.

power balance of each divertor region is simply written as

$$\frac{2}{\sqrt{m}} n_s T_s \left(\gamma_* T_s^{1/2} + k\Delta E \frac{R-1}{R} T_s^{-1/2} \right) \approx \frac{2}{7} \kappa_* \frac{T_0^{7/2} - T_s^{7/2}}{L_{SOL}/2 + L_{div}}, \quad (7)$$

where γ_* and κ_* are the heat transmission coefficient and the coefficient of the electron heat conductivity parallel to the magnetic field, $\kappa_{e\|} = \kappa_* T^{5/2}$, respectively. In Eq. (7), the first, the second term in LHS, and the RHS term denote the heat flux flowing to the divertor plate, the radiation integrated in the divertor region, and the conductive heat flux at the divertor throat, respectively. From Eqs. (6) and (7) with conditions of $0 \approx T_{sA} \ll T_{sB} \ll T_0$, a relation between T_{sA} and T_{sB} is derived as,

$$T_{sB} = \left(\frac{1 - f_{mA}}{1 - f_{mB}} \frac{k\Delta E(R-1)/R}{\gamma_*} \right)^2 \frac{1}{T_{sA}}. \quad (8)$$

Without the momentum loss ($f_{mA} = f_{mB} = 0$), T_{sB} largely increases when T_{sA} decreases near zero as shown at $R \approx 40$ in Fig. 4(a). With the momentum loss ($c_m = 1$), T_{sB} does not largely increases with decreasing T_{sA}. The mitigation of the asymmetry is easily found from Eq. (8) where f_{mA} increases and f_{mB} is nearly constant. When $T_{sA}/\Delta E$ decreases below about 0.5, the asymmetry with the momentum loss decreases compared to that without the momentum loss. The momentum loss increases the pre-sheath potential (see Fig. 1) as follows. The third term in RHS of the generalized Ohm's law in Eq. (1) is a contribution of the pressure gradient to the pre-sheath potential. The part of the potential drop due to the pressure gradient in the divertor region, $\delta\phi_{ps}$, is given as,

$$\delta\phi_{ps} = -\int_{div} \frac{1}{en} \frac{\partial nT}{\partial z} dz \approx \frac{n_0 T_0 - n_s T_s}{e n_s} = \frac{T_s}{e} \frac{2 + f_m}{1 - f_m}. \quad (9)$$

In Fig. 4(b), at the low-T_s side 'A', the momentum loss, f_m, increases and the pre-sheath potential, $\delta\phi_{ps}$, also increases. The increase in the pre-sheath potential due to the momentum loss is also found in the results of PARASOL [7]. At the low-T_s side, the thermoelectric sheath potential becomes small while the pre-sheath potential becomes large as illustrated in Fig. 1. On the other hand, at the high-T_s side, the momentum loss and the pre-sheath potential are not much changed. The change of the pre-sheath potentials decreases the potential difference between edges of the SOL region. The pre-sheath potential compensates the reduction of the sheath potential at the low-T_s side of an asymmetric equilibrium, and reduces the SOL current. Through the change of the pre-sheath potential, the momentum loss has a stabilizing effect on the thermoelectric instability and mitigates the asymmetry at the high-n_s divertor regime.

3.2. Effect of the momentum loss on the bifurcated structure of the equilibrium

We next consider cases where R is different between the divertor 'A' and 'B'. Fig. 5 shows a dependence of equilibrium values of $T_{sB}/\Delta E$ on R_B with and without the momentum loss where R_A is fixed to (a) 20 and (b) 35. The value of c_m is given as $c_m = 0$ and 1 for the cases without and with the momentum loss, respectively. The dependence of T_{sB} on R_B has a bifurcated structure indicated in Ref. [4], i.e., high-T_{sB} and low-T_{sB} stable equilibria exist and the middle equilibrium is unstable. In the both cases of $R_A = 20$ and 35, the difference between T_{sB} with and without the momentum loss more increases for larger R_B. Without the momentum loss, the high-T_{sB} stable equilibrium only remains for large R_B. In Fig. 5(b), $T_{sB}/\Delta E$ does not decrease below 1.4 for $R_A = 35$. On the other hand, with the momentum loss, the high-T_{sB} equilibrium disappears for smaller R_B and the low-T_{sB} one remains for larger R_B compared to the case without the momentum loss. In the case of $R_B = 35$ with the momentum loss, T_{sB} at the high-T_{sB} equilibrium decreases largely with increasing R_B compared with the case of $R_A = 20$. At the low-T_s side 'A' of the high-T_{sB} equilibrium in Fig. 5, the momentum loss in $R_A = 35$ is larger than that in $R_A = 20$ and the larger momentum loss more mitigates the asymmetry. The momentum loss

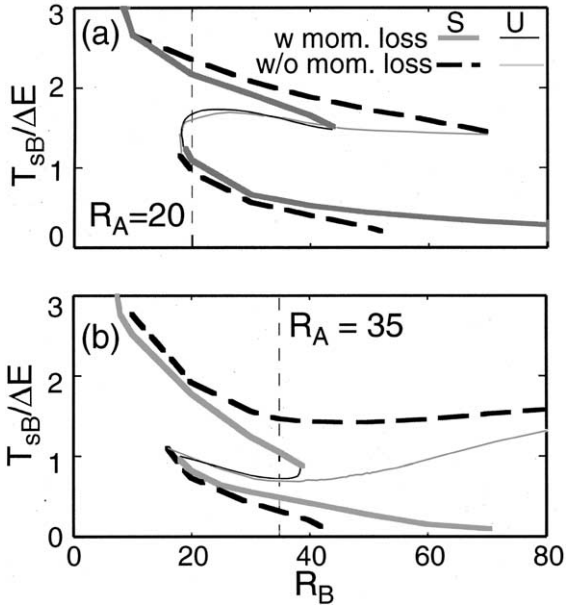

Fig. 5. Dependence of equilibrium values of $T_{sB}/\Delta E$ on R_B with (solid line) and without (broken line) the momentum loss where R_A is fixed to (a) 20 and (b) 35. Broad and thin line indicate stable (S) and unstable (U) equilibrium, respectively.

at the low-T_s and high-n_s side divertor is effective to lower the temperature at the high-T_s side divertor.

4. Summary

Asymmetric equilibria of divertor plasmas influenced by the thermoelectric potential and the momentum loss due to the CX have been studied by using a five-point model. A simple model for the CX momentum loss has been developed and introduced into the five-point model. The momentum loss becomes large when the divertor plasma temperature decreases below about 10 eV. At the low-T_s side of an asymmetric equilibrium, the increase of the pre-sheath potential due to the momentum loss compensates the reduction of the thermoelectric sheath potential. Through the change of the pre-sheath potential, the momentum loss has a stabilizing effect on the thermoelectric instability and mitigates the asymmetry at the high-n_s divertor regime. The momentum loss at the low-T_s and high-n_s side divertor is effective to lower the temperature at the high-T_s side divertor.

Acknowledgements

The authors would like to thank Dr N. Asakura and Professor A. Hatayama for fruitful discussions. We are grateful to Dr T. Ozeki for his encouragement.

References

[1] B. LaBombard et al., J. Nucl. Mater. 241–243 (1997) 149.
[2] N. Hayashi, T. Takizuka, A. Hatayama, M. Ogasawara, Nucl. Fusion 38 (1998) 1695.
[3] N. Hayashi, T. Takizuka, A. Hatayama, M. Ogasawara, J. Nucl. Mater. 266–269 (1999) 526.
[4] N. Hayashi, T. Takizuka, K. Shimizu, Contribution Plasma Phys. 40 (2000) 387.
[5] T. Takizuka, M. Hosokawa, K. Shimizu, Trans. Fusion Technol. 39 (2001) 111.
[6] M.F.A. Harrison, P.J. Harbour, E.S. Hotston, Nucl. Technol. Fusion 3 (1983) 432.
[7] T. Takizuka, M. Hosokawa, K. Shimizu, J. Nucl. Mater. 290–293 (2001) 753.